International Conference on Space Optics—ICSO 2012

Ajaccio, Corse

9–12 October 2012

Edited by Bruno Cugny, Errico Armandillo, and Nikos Karafolas

Effects of proton irradiation on thin-film materials for optical filters

Salvatore Scaglione

Angela Piegari

Anna Sytchkova

Milko Jakšić

International Conference on Space Optics — ICSO 2012, edited by Bruno Cugny, Errico Armandillo, Nikos Karafolas
Proc. of SPIE Vol. 10564, 105642A · © 2012 ESA and CNES · CCC code: 0277-786X/17/$18 · doi: 10.1117/12.2309132

Effects of proton irradiation on thin-film materials for optical filters

Salvatore Scaglione, Angela Piegari, Anna Sytchkova
ENEA, Optical Coatings Laboratory,
Rome, Italy
salvatore.scaglione@enea.it

Milko Jaksic
Rudjer Boskovic Institute,
Zagreb, Croatia
jaksic@irb.hr

***Abstract*— The behaviour of interference optical filters for space applications has been investigated under low energy proton irradiation. In order to understand the behaviour of the interference coating subjected to proton irradiation, the interaction of protons with coating and substrate was simulated by the SRIM code. A beam of protons of 60 KeV with an integrated fluence of 10^{13} p^+/cm^2 was used. The spectral transmittances of fused silica, TiO_2 and HfO_2 single layers and interference coatings were measured before and after irradiation and, according to simulations, no significant effects were detected in the visible-near infrared spectrum, while some variations appeared at shorter wavelengths.**

Keywords - optical coating, proton irradiation, SRIM

I. INTRODUCTION

The irradiation of protons coming from the solar wind, is one of the reasons for the degradation of the optical components inside the instrumentation on-board of the in-orbit spacecrafts [1]. Low energy protons, 50-60 keV, seem to be more effective for the deterioration of the coating optical response, with respect to 30 MeV protons that have a negligible effect on the coating degradation [2].

Both experiments at laboratory level and simulation of the protons effect on the material can be useful for adopting suitable design and materials with the aim to limit the low energy proton damage.

This work is dedicated to proton irradiation of single layer materials and multilayer interference filters. After description of the filter optical performance, the SRIM code [3] simulation of proton interaction with matter is reported. Finally the results of the irradiation test are analysed.

II. EXPERIMENTAL

A. Sample preparation

The samples, irradiated by the proton beam, were manufactured by electron gun evaporation (Balzers, mod.BAK 640) equipped with an end-Hall ion source (Commonwealth Scientific Corporation, mod. Mark I), the energy of the Ar ion beam is between 40 eV and 150 eV. The vacuum chamber was evacuated by a cryopump at a back-pressure of $2\text{-}4\cdot10^{-6}$ Pa whereas the working pressure during the deposition process was 10^{-2} Pa.

In Table I the samples manufactured for low energy proton irradiation are listed.

TABLE I.

Sample		
	Design	***Material (thickness)***
#1	substrate	Fused silica (1 mm)
#2	Single layer	HfO_2 (690 nm)
#3	Single layer	TiO_2 (720 nm)
#4	Fabry-Perot $[(HL)^7\ HH\ (LH)^7]$	$L^a=SiO_2$, $H^b=HfO_2$, λ_0=316 nm
#5	Double Cavity $[(HL)^4\ HH\ (LH)^4\ L\ (HL)^4\ HH\ (LH)^4]$	$L^a=SiO_2$, $H^b=TiO_2$, λ_0=777 nm

λ_0 reference wavelength, a. L low index layer, SiO_2; b. H high index layer, TiO_2 or HfO_2.

B. Low energy proton irradiation

Tests with low-energy protons were carried out at the accelerator facility of the Rudjer Boskovic Institute, (Zagreb, Croatia). In order to obtain 60 keV of average proton energy, a beam of 400 keV protons was slowed down by transmission through an aluminum foil of appropriate thickness. A total fluence of 10^{13} p+/cm^2 was ensured.

C. Optical measurements

The transmittance measurements were performed by a commercial spectrophotometer (Perkin Elmer, mod. Lambda950). A homemade sample holder was manufactured to reposition the samples, before and after the proton irradiation, with the accuracy needed to ensure the repeatability of the transmittance measurements. In Fig.1, two different transmittance curves performed by removing and repositioning the fused silica sample are reported. The same procedure was used for all coatings.

D. p^+ irradiation simulation

The simulation of the proton irradiation was performed by a code based on the statistics of Montecarlo method [3] named SRIM (Stopping and Range in Ion Matter, vers. 2012 pro). A number of 10^4 ions was considered suitable to obtain reliable results.

After the p^+ irradiation simulations, and to interpret the measurement results, the optical transmittance of the samples was calculated (TfCalc software, vers. 3.5.15) with the hypothesis of some induced changes in the layer materials.

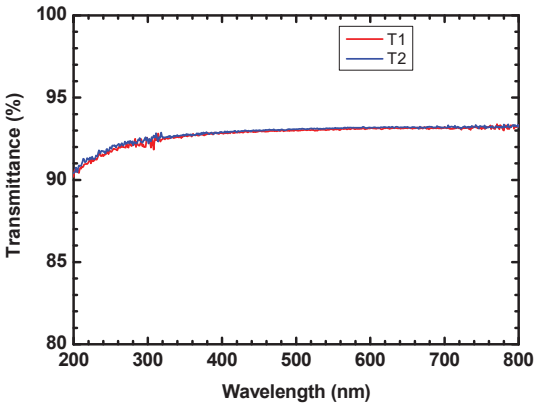

Figure 1. Comparison of the spectral transmittance curves of the same fused silica substrate, to verify the measurement repeatability.

III. Results and Discussion

In Fig.2 the transmittance curves of fused silica (#1), measured before and after the proton irradiation, are compared.

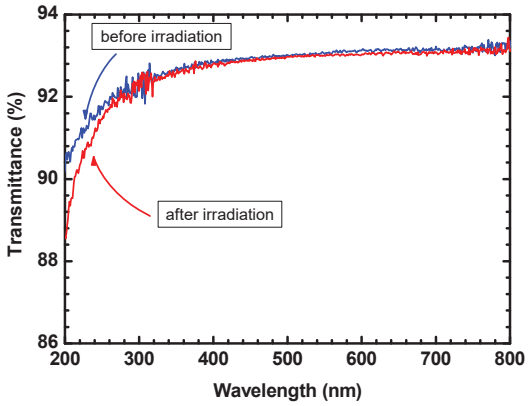

Figure 2. Transmittance curves of fused silica substrate (#1), before and after the proton irradiation.

After the irradiation, the transmittance decreases for wavelengths shorter than 300 nm whereas in the visible-near infrared spectral region the protons have negligible effect on the optical response. On the contrary, the transmittance of the titanium oxide and hafnium oxide layers (deposited on fused silica) doesn't change after the irradiation. In Figs. 3 and 4 these results are shown, in both cases the measurements were repeated several times to verify their reliability.

The interference coatings of Table I, samples #4 and #5, are composed by a sequence of low and high refractive index layers and any change of their optical properties, due the operating conditions, produces some modification of the whole optical response. In the Figs. 5, 6 and 7 the filter transmittances before and after the proton irradiation are reported. Both coatings exhibit a decrease in the transmittance values at short wavelengths after the proton irradiation.

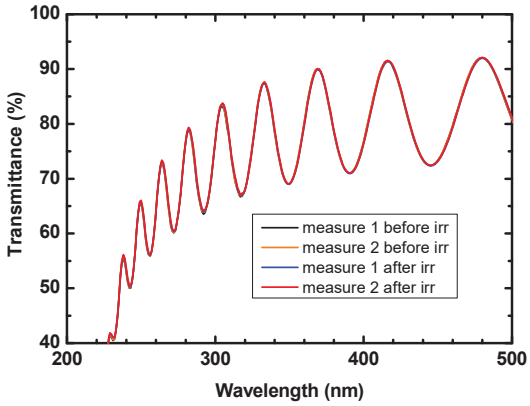

Figure 3. Transmittance curves of HfO_2 layer (#2), before and after the proton irradiation.

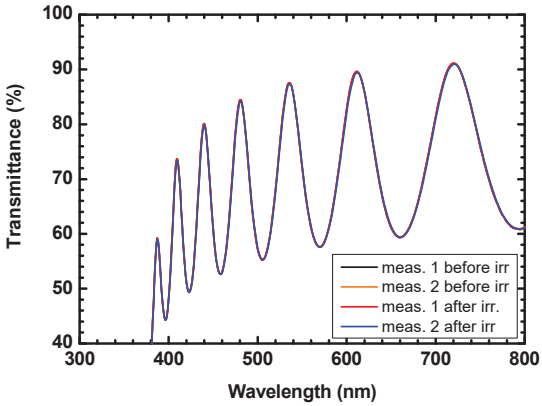

Figure 4. Transmittance curves of TiO_2 layer (#3), before and after the proton irradiation.

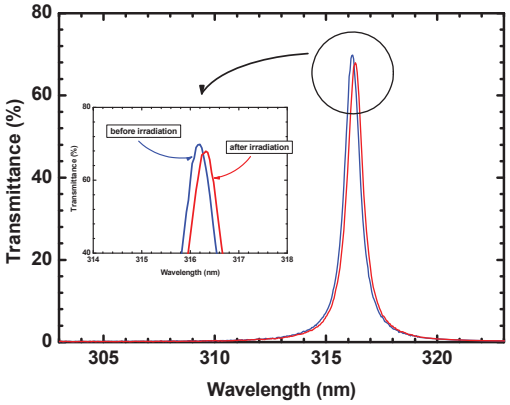

Figure 5. Transmittance curves of Fabry-Perot narrow-band filter (#4), before and after the proton irradiation.

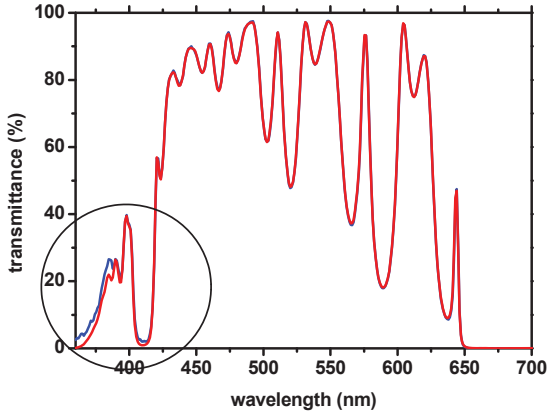

Figure 6. Transmittance curves of the Double Cavity narrow-band filter (#5) centered at 777 nm, before and after the proton irradiation.

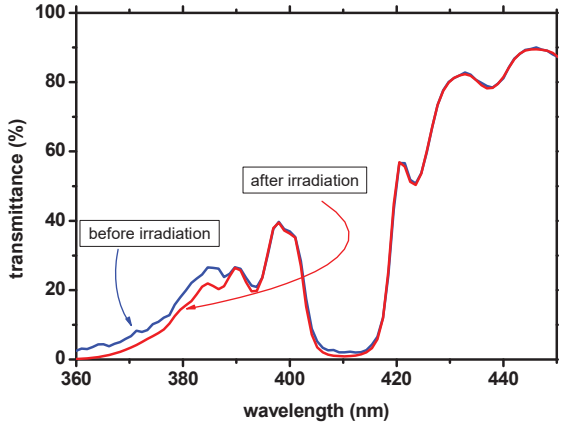

Figure 7. Transmittance curves of the ultraviolet range of Fig 6.

By analyzing the Figs. 2-4, it can be observed that the fused silica substrate (SiO_2) is the material that suffers most damage when subjected to 60 keV proton irradiation. As can be seen in the Figs. 5-7, this effect induces changes in the transmittance of the interference coatings where the SiO_2 material is used.

In order to understand the effect of the protons on the SiO_2 layers, the irradiation was simulated by the SRIM code.

A. *SRIM simulation of 60keV protons*

During the collisions, the protons are able to displace the atoms of the target from their equilibrium position and SRIM is able to follow the trajectory of the atoms calculating the number of atoms which become at rest in the interstitial position and in the substitutional configuration.

1) *Fused silica (#1)*

In Fig. 8 the simulation of ions and recoils collision cascade for the fused silica substrate is reported. The ion average range, R_{ion}, of the protons is 578.2 nm and the collision cascade is approximately effective up to 800 nm.

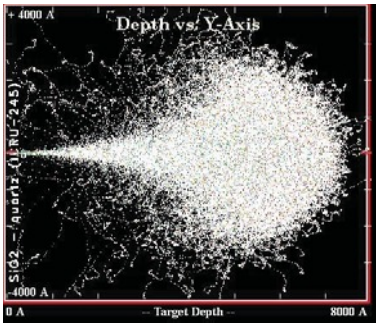

Figure 8. Distribution of ions and recoils in a SRIM simulation for the fused silica substrate (#1).

The distribution of oxygen vacancies with the depth, i.e. the oxygen atoms in the interstitial configuration, is reported in Fig.9

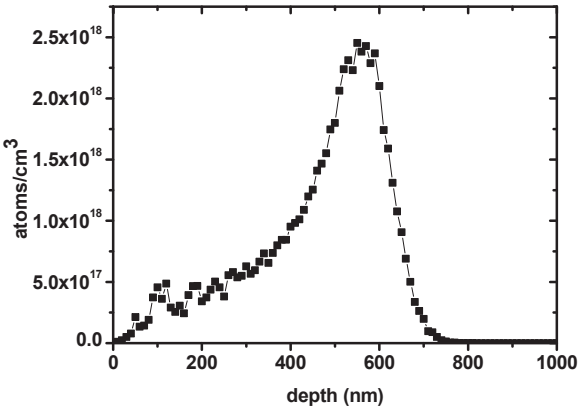

Figure 9. Oxygen vacancies distribution in fused silica substrate, SRIM simulation.

The units of the plot ordinate in SRIM simulation are $(atoms/cm^3)/(atoms/cm^2)$ and, multiplying these units by the ion dose ($p^+=10^{13}$ protons/cm^2), the ordinate converts directly into a density distribution with units of $atoms/cm^3$.

In the following, the calculations of the optical response of the interference coatings are performed in the hypothesis that only the low refractive index layers, SiO_2, subjected to protons irradiation, are responsible for the change in the transmittance curves.

In this frame, it can be considered that the vacancies are generated removing the oxygen atoms from the equilibrium position and the average stoichiometry of the material region interested to the collision cascade is altered as:

$$Si{:}O_2 = Si{:}O + O \qquad (1)$$

As a consequence, after the proton irradiation, the low refractive index layers can be considered as a mixing of SiO_2 and SiO. The relative concentrations depend on the target depth.

The dispersion curves of the refractive index of SiO_2 and SiO used to generate the mixed L layers are reported in Fig.10 [4].

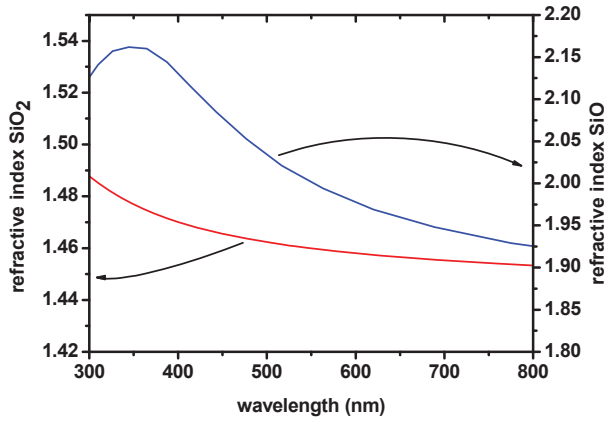

Figure 10. Refractive indexes of SiO_2 and SiO.

The extinction coefficient, k, of SiO is reported in Fig.11. The k values of SiO_2 ($k<10^{-4}$) do not influence the optical performance of the analyzed interference coatings and for this reason its dispersion curve is not reported.

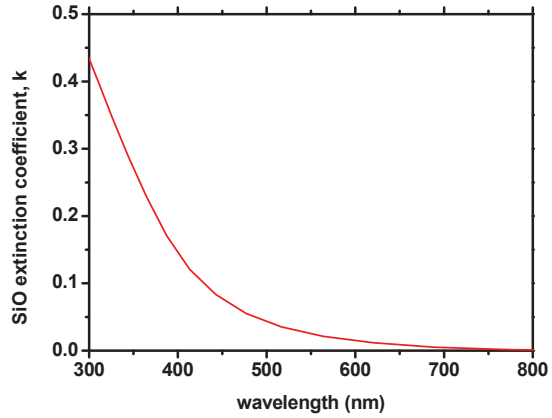

Figure 11. SiO extinction coefficient.

The transmittance of the fused silica substrate (#1) is calculated dividing the SRIM simulated region in 20 layers with a different percentages of SiO content. In Fig. 12 the relative percentage of SiO content with the depth is reported. In Fig. 13, the transmittance curves of stoichiometric SiO_2, i.e. SiO content equal zero, and p^+ SRIM simulated layer (SiO content of Fig.12) are reported.

The shapes of the calculated transmittance curves of Fig. 13 are very similar to the experimental curves reported in Fig.2.

In case of samples #2 and #3, the thickness of such coatings prevent the protons to reach the substrate.

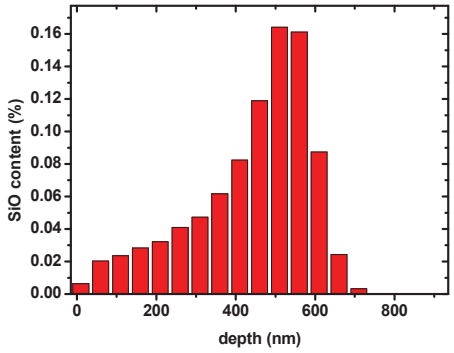

Figure 12. Percentage of SiO in the layers near the surface of irradiated fused silica sample.

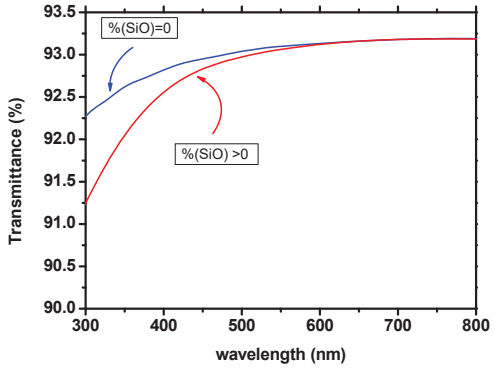

Figure 13. Comparison of the transmittance curves of fused silica calculated with the content of SiO reported in Fig. 12 .

2) Fabry-Perot filter (#4)

The same procedure described above was used for both the Fabry-Perot narrow-band filter (FP-NBF, #4) and Double Cavity narrow-band filter (DC-NBF, #5). The optical degradation observed in Fig.5 is ascribed to the SiO_2 layers subjected to the proton irradiation, in fact the HfO_2 layers seem not to be damaged by the proton irradiation (see Fig.3).

In Fig.14, the SRIM simulation of ions and recoils distributions is shown for the FP-NBF coating. As can be seen, the protons are stopped in the first 650 nm of the filter whereas the remaining 730 nm are not interested to the collision cascade (the total thickness is 1380 nm). The SRIM simulation layout is:

$$p^+(60keV) \Rightarrow (HL)^7\ HH\ (HL)^7$$

The thickness, d, of the layers depends on the reference wavelength, in the case of Fig.14, $d_L(SiO_2)$ = 53 nm and $d_H(HfO_2)$ = 39 nm.

In Fig. 15, the density of the oxygen vacancies with the depth for the L layers is reported. The SiO relative percentage with the L layer number is reported in Fig.16.

The transmittance of the Fabry-Perot filter is shown in Fig.17 and was calculated changing the SiO_2/SiO ratio in the first seven L layers of the filter.

The decrease of the transmittance in SRIM simulated filter appears similar to the experimental curves of Fig.5. On the contrary, the slight wavelength shift noticed in Fig.5 was not noticed in the transmittance curves of Fig. 17.

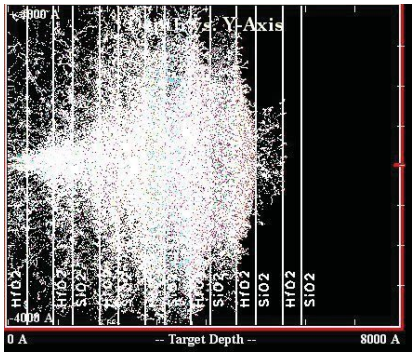

Figure 14. Distribution of ions and recoils in a SRIM simulation of the Fabry-Perot narrow band filter (#4).

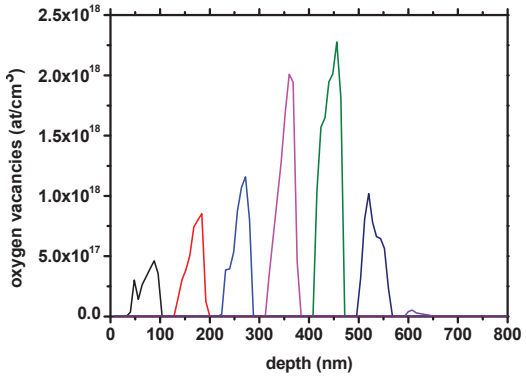

Figure 15. Oxygen vacancies distribution in the SiO_2 layers of the Fabry-Perot narrow band filter.

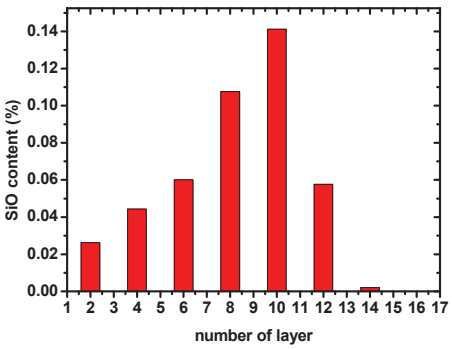

Figure 16. Percentage of SiO in the layers near the surface of the irradiated Fabry-Perot narrow band filter.

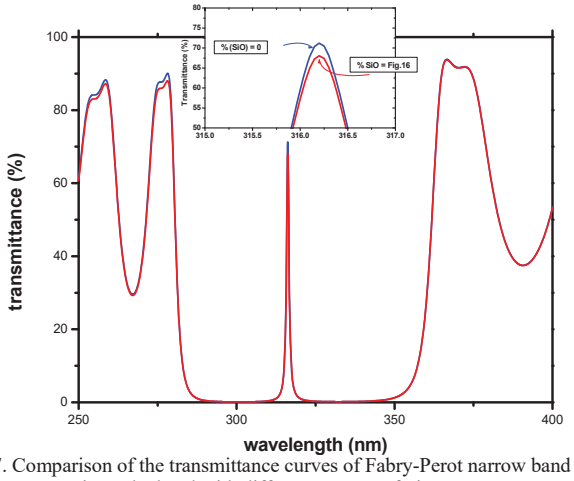

Figure 17. Comparison of the transmittance curves of Fabry-Perot narrow band coating calculated with different content of SiO.

3) Double Cavity Narrow Band Filter

Different L and H thicknesses were used for the SRIM simulation of the filter DC-NBF. In particular, $d_L(SiO_2)$ = 133.7 nm and $d_H(TiO_2)$ = 81 nm.

In Fig.18 the SRIM simulation of sample #5 is reported. Because of the thicker L layers with respect to the Fabry-Perot filter (sample #4), in this case, the layers interested to the collision cascade are only three.

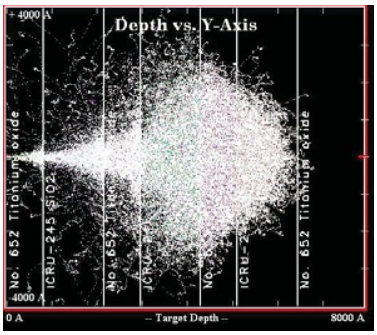

Figure 18. Distribution of ions and recoils in a SRIM simulation of the Double Cavity narrow band filter (#5).

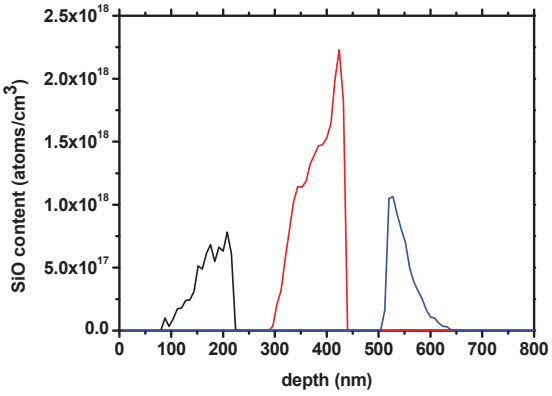

Figure 19. Oxygen vacancies distribution in the SiO_2 layers of the Double Cavity narrow band filter.

In Figs. 19 and 20 the oxygen vacancies with the depth and the percentage of SiO are respectively reported.

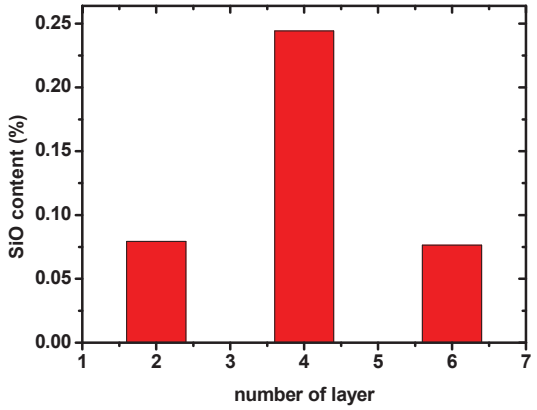

Figure 20. Percentage of SiO in the layers near the surface of the irradiated Double Cavity narrow band filter.

The transmittance curves of the Double Cavity filter calculated varying the stoichiometry of the first three L layers are shown in Fig.21. The transmittance decrease that can be seen in Fig.21 is quite in agreement with the experimental curves shown in Fig.7, even though appears less pronounced.

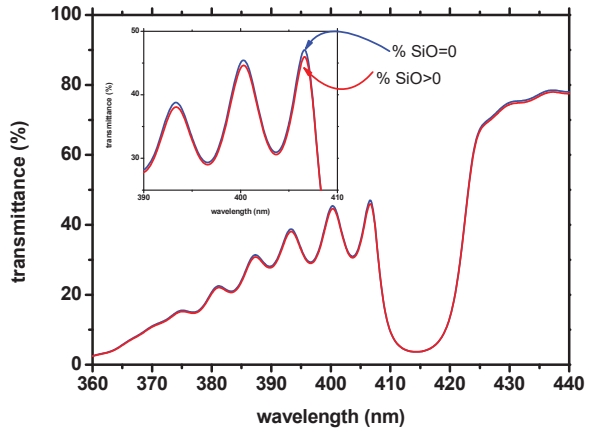

Figure 21. Comparison of the transmittance curves of the Double Cavity narrow band filter calculated with the SiO content of Fig.20.

In general, the calculated transmittance curves seem to be in agreement with the hypothesis described by the relation 1, i.e. each oxygen atom removed from the equilibrium position generates a SiO molecule. The idea that the SiO_2 material is more sensitive to the proton irradiation is confirmed by the Figs. 3 and 4 where no variation of the transmittance curves is noticed.

IV. Conclusions

Low energy protons coming from the solar wind can damage the materials of the coated optical components operating on-board of spacecraft instrumentation. Silicon oxide, titanium oxide, hafnium oxide and two interference coatings were irradiated by 60 keV protons and measured before and after the irradiation process. The transmittance of the silicon oxide decreases at short wavelength (UV) indicating a change in the material stoichiometry. This effect was simulated by the SRIM code and the number of vacancies obtained from the simulation was used to calculate the relative concentration of SiO. Substituting the SiO_2 layer with a mixing of SiO and SiO_2, the transmittance curves were calculated. The experimental transmittances of the coatings after the proton irradiation and those calculated with a mixing of SiO/SiO_2 in the low refractive index layers are in agreement.

Acknowledgment

The authors are grateful to I. Di Sarcina, M.L. Grilli, F. Menchini, D. Zola and M. Karlusic for the manufacturing, irradiation and measurements of samples.

References

[1] M.G. Pelizzo, Alain Jody Corso, Paola Zuppella, D.L. Windt, G. Mattei, P. Nicolosi, “Stability of extreme ultraviolet multilayer coatings to low energy proton bombardment”, Optics Express, vol. 19, No 16, pp. 14838-14844, August 2011.

[2] A. Piegari, I. Di Sarcina, M. L. Grilli, F. Menchini, S. Scaglione, A. Sytchkova, “Optical performance of narrow-band transmittance filters under low-and high-energy proton irradiation”, Proc. SPIE, vol. 8168, September 2011.

[3] J. F. Ziegler and J.P.Biersack, www.srim.org

[4] http://www.filmetrics.com/refractive-index-database/